A simple model to analytically assess the SH seismoelectric response of the vadose zone

L.B. Monachesi [1], F.I. Zyserman [2] and L. Jouniaux [3]

[1] Instituto de Investigación en Paleobiología y Geología, Universidad Nacional de Río Negro y CONICET, Av. Roca 1242, Gral. Roca, Río Negro, Patagonia Argentina;
email: lmonachesi@unrn.edu.ar
[2] Facultad de Ciencias Astronómicas y Geofísicas, Universidad Nacional de La Plata y CONICET. Paseo del Bosque s/n, B1900FWA La Plata, Argentina;
email: zyserman@fcaglp.unlp.edu.ar
[3] Institut de Physique du Globe de Strasbourg, EOST, UdS-CNRS UMR 7516, Université de Strasbourg, 5 rue René Descartes, 67084 Strasbourg, France;
email: l.jouniaux@unistra.fr

ABSTRACT

In this work an analytical solution of the seismoelectric conversions generated in the vadose zone, when this region is traversed by a pure SH wave, is derived. The considered model assumes a one-dimensional soil constituted by two homogeneous media in contact at the water table, and a shearing force located at the earth's surface as the wave source. The model also considers that the electroosmotic feedback can be neglected in Biot's equations, as it is usually assumed. The upper medium represents a partially saturated porous rock whose porous space contains the minimum amount of water, while the lower medium is completely saturated with water, representing the saturated zone. The analytical expressions for both electric and magnetic fields are analyzed for a hypothetical scenario. The main result shows that a sharp contrast in water saturation at the water table can induce strong interfacial responces in both fields.

INTRODUCTION

Seismoelectromagnetic methods were developed to investigate hydrogeological reservoirs (Dupuis et al., 2009; Schakel et al., 2012; Warden et al., 2013), specially in arid environments (Valuri et al., 2012), and hydrocarbon reservoirs (Zyserman et al., 2012; Guan et al., 2013; Zyserman et al., 2015). The seismoelectric method aims at combining the sensitivity of the electric methods to the fluid content with the spatial resolution of the seismic method. Most of the studies were developed considering a single saturating fluid at full saturation. It was only in the few last years that attempts to introduce partial saturation in seismoelectrics/electroseismics have been undertaken (Warden et al., 2013; Zyserman et al., 2015). Recently Zyserman et al. (2017) studied the seismoelectric conversions generated in the vadose zone when this region is traversed by a

pure shear SH wave, instead of a pure compressional P-wave as usually studied. The numerical results showed that the seismoelectric conversions induced by a shear wave source lead to an electric interfacial response of about three orders of magnitude larger than the coseismic signal amplitude, leading to a possible detection of the water table by seismoelectromagnetic measurements. In the present work, these seismoelectromagnetic conversions induced in the vadose zone are analytically derived for a simple one-dimensional model.

THEORETICAL BACKGROUND

Let's assume a porous medium constituted by two regions in the $x - z$ plane, being z the vertical axis (positive downwards) and x the horizontal axis, as it is schematically depicted in Fig. 1. The origin of the z coordinates is located at the surface, and both

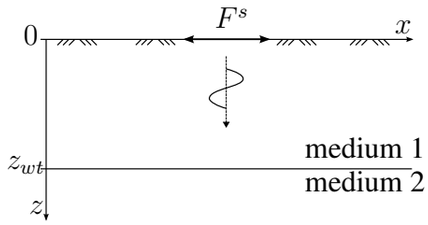

Figure 1. Schematic representation of the seismic shear plane wave travelling downwards in a two-layer one-dimensional system.

regions are in contact at $z = z_{wt}$ (the depth to the water table). The upper region ($0 < z < z_{wt}$) labeled as 1, represents a partially saturated porous rock whose porous space contains the minimum amount of water (residual content). This space mimics the so called vadose zone under the assumption that the water saturation remains constant with depth. The lower region ($z > z_{wt}$), labeled as 2, is completely saturated by water, and represents the saturated zone below the water table. We model the electromagnetic response to seismic waves generated by a shear source using the equations derived by Pride (1994). In particular we assume that the source of the system is a shearing force located at the earth's surface, parallel to the x axis acting on a horizontal infinite plane (see Fig.1). Under these assumptions both solid and fluid phases can only undergo displacements in the x axis direction, with amplitudes depending only on depth z; no compressional waves can arise in this model and spherical spreading and Fresnel zone effects are not accounted for. If we also consider that the electroosmotic feedback can be neglected in Biot's equations, as it is usually assumed for frequencies in the range of interest for shallow seismoelectric surveys (10 Hz to 1 kHz) (Haines and R.Pride, 2006), Pride's electromagnetic equations can be written in the space-frequency domain,

assuming a $e^{i\omega t}$ time dependence, as follows

$$\sigma E_x - \frac{\partial H_y}{\partial z} = i\omega \frac{\eta}{\kappa} L_0 u_{f,x} = j_v, \tag{1}$$

$$\frac{\partial E_x}{\partial z} + i\omega\mu_0 H_y = 0, \tag{2}$$

$$-\omega^2 \rho_b u_{s,x} - \omega^2 \rho_f u_{f,x} = G \frac{\partial^2 u_{s,x}}{\partial z^2}, \tag{3}$$

$$-\omega^2 \rho_f u_{s,x} - \omega^2 g_0 u_{f,x} + i\omega \frac{\eta}{\kappa} u_{f,x} = 0. \tag{4}$$

In these equations, E_x and H_y are the electric and magnetic fields, respectively, and $u_{s,x}$ and $u_{f,x}$ are the solid and average relative fluid displacements, respectively. From now on, for the sake of simplicity, we denote $E \equiv E_x$, $H \equiv H_y$, $u_s \equiv u_{s,x}$ and $u_f \equiv u_{f,x}$. The remaining parameters in Eqs. (1)-(4) are the electric conductivity σ, fluid viscosity η, hydraulic permeability κ, electrokinetic coupling L_0, vacuum magnetic permeability μ_0, bulk density ρ_b, fluid density ρ_f, Biot's low frequency inertial coupling coefficient g_0 and shear modulus of the solid frame G. The right hand side in Eq. (1) is the electric current density, source of the electromagnetic signals, and can be named the viscous current density j_v, whereas σE_x is the conduction current.

Suppose that a shear seismic plane wave is generated at $z = 0$, traveling downwards from the surface to the water table (see Fig.1). If the wave is harmonic with angular frequency ω and polarized in the x axis direction, the solid and relative fluid displacements in medium 1, $u_{s,1}$ and $u_{f,1}$ can be written as:

$$u_{s,1} = U_{s,1} e^{i\lambda_1 z} \text{ and } u_{f,1} = U_{f,1} e^{i\lambda_1 z}, \tag{5}$$

where λ_1 is the wave number of medium 1, $v_1 = \omega/|Re(\lambda_1)|$ is the S-wave phase velocity, and $U_{s,1}$ and $U_{f,1}$ are the amplitudes of the solid and relative fluid displacements at $z = 0$, respectively. Following the same reasoning the corresponding displacements in medium 2 can be expressed as:

$$u_{s,2} = U_{s,2} e^{i\lambda_2 (z - z_{wt})} \text{ and } u_{f,2} = U_{f,2} e^{i\lambda_2 (z - z_{wt})}. \tag{6}$$

Using these expressions in Eqs. (3) and (4) the following relations can be obtained (Pride, 2005):

$$u_{f,1} = -\frac{\rho_{f,1}}{g_{0,1} + \frac{i\eta_1}{\omega\kappa_1}} u_{s,1} \quad \text{and} \quad u_{f,2} = -\frac{\rho_{f,2}}{g_{0,2} + \frac{i\eta_2}{\omega\kappa_2}} u_{s,2}. \tag{7}$$

Now, let's assume that the solid matrix of the porous medium is the same for both regions (they only differ in fluid content). Then, the wave will pass through the interface with no reflections (Liu and Greenhalgh, 2014) and the amplitude of the solid displacement at $z = z_{wt}$ will be the same for both incident and transmitted waves. This allows to write $u_{s,2}(z_{wt}) = u_{s,1}(z_{wt})$, that is, according to Eqs. (5) and (6), $U_{s,1} e^{i\lambda_1 z_{wt}} = U_{s,2}$.

Moreover, being the solid matrix the same for both regions, the hydraulic permeabilities will also be the same, so we can write $\kappa_1 = \kappa_2 = \kappa$.
The viscous current density j_v generated by the relative fluid motion can be obtained for both media as follows (see Eq. (1)):

$$j_{v,1} = i\omega\eta_1 \frac{L_{0,1}}{\kappa} u_{f,1} = \frac{\omega^2 \rho_{f,1} L_{0,1}}{1 + i\omega g_{0,1} \kappa \eta_1^{-1}} U_{s,1} e^{i\lambda_1 z} = J_1^{wt} e^{i\lambda_1 (z - z_{wt})}, \tag{8}$$

$$j_{v,2} = i\omega\eta_2 \frac{L_{0,2}}{\kappa} u_{f,2} = \frac{\omega^2 \rho_{f,2} L_{0,2}}{1 + i\omega g_{0,2} \kappa \eta_2^{-1}} U_{s,2} e^{i\lambda_2 (z - z_{wt})} = J_2^{wt} e^{i\lambda_2 (z - z_{wt})}, \tag{9}$$

being J_1^{wt} and J_2^{wt} the amplitudes of the current density at the water table in medium 1 and in medium 2, respectively. Note that, being the water content profile discontinuous at $z = z_{wt}$, the relative fluid displacement will be discontinuous, and so the current density.
Now, let's explore the influence of the current density as a source of electromagnetic fields. Taking the first derivative with respect to z in Eq. (2), replacing the resulting expression in Eq. (1) and using Eqs. (8) and (9), the following equations are obtained for the electric field

$$\frac{d^2 E}{dz^2} + {k_1}^2 E = i\omega\mu_0 J_1^{wt} e^{i\lambda_1 (z - z_{wt})}, \quad 0 \leq z < z_{wt}, \tag{10}$$

$$\frac{d^2 E}{dz^2} + {k_2}^2 E = i\omega\mu_0 J_2^{wt} e^{i\lambda_2 (z - z_{wt})}, \quad z > z_{wt}, \tag{11}$$

being $k_* = \sqrt{i\omega\mu_0\sigma_*}$ $(* = 1, 2)$. The general solutions for Eqs. (10) and (11) are respectively given by

$$E(z,\omega) = A_1 e^{-ik_1 z} + B_1 e^{ik_1 z} + \frac{k_1^2 J_1^{wt} e^{i\lambda_1 (z - z_{wt})}}{(k_1^2 - \lambda_1^2)\sigma_1}, \quad 0 \leq z < z_{wt}, \tag{12}$$

$$E(z,\omega) = A_2 e^{-ik_2 z} + B_2 e^{ik_2 z} + \frac{k_2^2 J_2^{wt} e^{i\lambda_2 (z - z_{wt})}}{(k_2^2 - \lambda_2^2)\sigma_2}, \quad z > z_{wt}, \tag{13}$$

where A_1, B_1, A_2 and B_2 are frequency dependent complex constants. The magnetic field H can be obtained from E using Eq. (2), leading to

$$H(z,\omega) = \frac{k_1}{\omega\mu_0} \left(A_1 e^{-ik_1 z} - B_1 e^{ik_1 z} \right) - \frac{i\lambda_1 J_1^{wt} e^{i\lambda_1 (z - z_{wt})}}{k_1^2 - \lambda_1^2}, \quad 0 \leq z < z_{wt}, \tag{14}$$

$$H(z,\omega) = \frac{k_2}{\omega\mu_0} \left(A_2 e^{-ik_2 z} - B_2 e^{ik_2 z} \right) - \frac{i\lambda_2 J_2^{wt} e^{i\lambda_2 (z - z_{wt})}}{k_2^2 - \lambda_2^2}, \quad z > z_{wt}. \tag{15}$$

The unknown constants A_1, B_1, A_2 and B_2 should be obtained by imposing conditions on the interface of both media at $z = z_{wt}$, and at the boundaries of the system ($z = 0$ and $z \to \infty$). First, if we choose k_2 such that $Im(k_2) < 0$, then B_2 must vanish in

order to avoid the divergence of the electromagnetic fields when $z \to \infty$. If the earth surface is in contact with air, and if we assume that the air is dielectric, then the amplitude of the electric field must be constant for $z \leq 0$ in order to avoid its divergence when $z \to -\infty$, and in virtue of Eq. (2) $H = 0$ for $z < 0$. Establishing the continuity condition of the magnetic field at $z = 0$ and for both fields at $z = z_{wt}$, the remaining constants A_1, B_1 and A_2 can be obtained. Once the fields $E(z, \omega)$ and $H(z, \omega)$ are known for a given depth z, the time variations of these fields at that depth are obtained by inverse Fourier transform of the product between the spectra of the source, $F(\omega) = \mathcal{F}\{f(t)\}$ (being $f(t)$ the time signature of the source) and the corresponding field, that is, $E(z,t) = \mathcal{F}^{-1}\{E(z,\omega)F(\omega)\}$ and $H(z,t) = \mathcal{F}^{-1}\{H(z,\omega)F(\omega)\}$.
Note that the third terms of Eqs. (12)-(15) have wave numbers λ_*, corresponding to a wave propagation at seismic velocities. These terms are interpreted as the electromagnetic coseismic responses. On the other hand, the first two terms in these equations have wave numbers k_*, which correspond to electromagnetic signals. These terms account for the interfacial responses originated at the surface and at the water table, as we show below. In the following section a hypothetical example is proposed to analyze the electromagnetic responses predicted by the derived analytical solution.

RESULTS AND DISCUSSION

To illustrate the field responses predicted by the derived analytical solution we consider the physical properties listed in Table 1. Both the porous matrix properties and the effective properties of the media are computed for a loamy sand following Zyserman et al. (2017). The water table is assumed to be located at 25 m below the surface, and as the time signature of the seismic source $f(t)$ we use a Ricker wavelet with peak frequency $f_c = 120$ Hz, the peak amplitude for the Ricker wavelet (located at $t = 8 \times 10^{-3}$ s) is set to 1 and the amplitude of the solid displacement at the surface is $U_{s,1} = 1$ m. Note this is not a realistic value for a field source but it is appropriated for a qualitative analysis.

Table 1. Material properties employed in the proposed example.

Properties of the porous matrix		
Permeability, κ [m^2]		4.02×10^{-12}
Shear modulus, G [GPa]		7.6
Effective Properties	medium 1	medium 2
Water Saturation, S_w	0.3	1
Fluid density, ρ_f[Kg m^{-3}]	308.9	1027
Fluid viscosity, η [Pa s]	6.03×10^{-5}	10^{-3}
Biot's inertial coefficient, g_0[Kg m^{-3}]	2865.5	9525.7
Electrical conductivity, σ [S m^{-1}]	1.13×10^{-4}	10^{-2}
Electrokinetic coupling, L_0 [A Pa^{-1}m^{-1}]	2.02×10^{-10}	4.8×10^{-10}

The time variation of the solid displacement and the current density, together with the interfacial and coseismic responses of the electric and magnetic fields are plotted in Fig. 2 for 11 different depths measured from the surface. As can be seen, the solid displace-

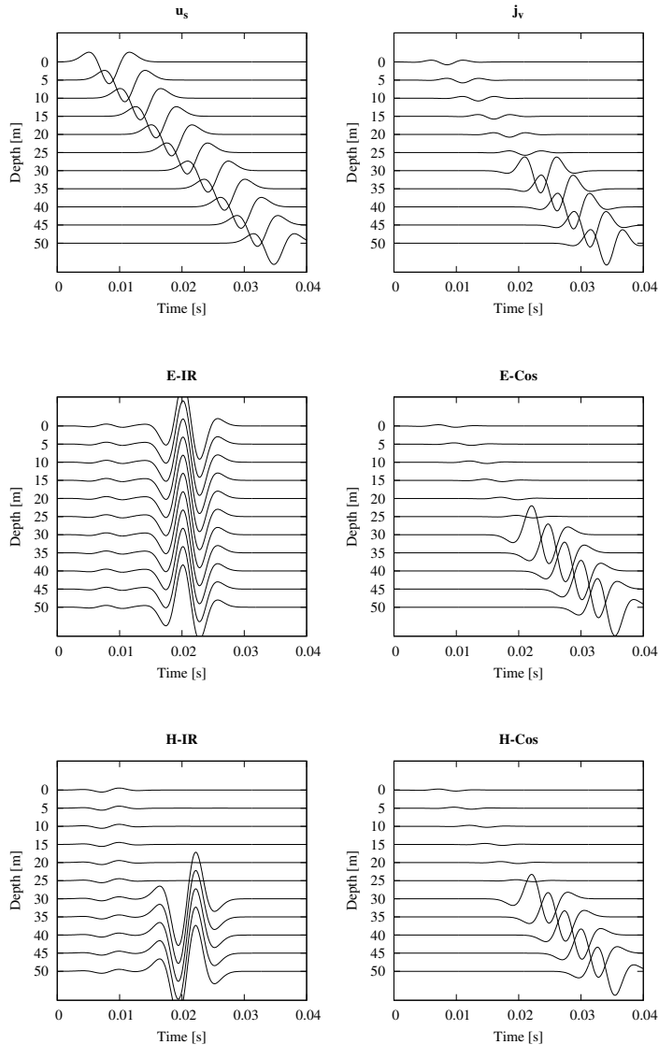

Figure 2. Time variation of u_s (top left), j_v (top right), E-IR (central left), E-Cos (central right), H-IR (bottom left), H-Cos (bottom right).

ment u_s induced by the source at the surface travels downwards with fairly constant seismic velocity and amplitude. The current density j_v follows the same time dependence as u_s but with a sharp increase of amplitude when the water table is reached. This was expected given the sharp contrast in water saturation, which in turn produces a corresponding jump in u_f.

The interfacial response of the electric field E-IR shows two events originated at two different times. The first one is attributed to an interfacial response originated at the surface, and the second one corresponds to the interfacial response originated at the water table. As can be seen, the amplitudes of both signals are markedly different. The coseismic response of the electric field E-Cos shows the same behavior as the current density, being its amplitude higher below the water table. Although it can not be interpreted from the figure, the amplitude of the interfacial response at the water table is three orders of magnitude higher than the amplitude of the coseismic field below the water table.

Concerning the interface response of the magnetic field H-IR, the one corresponding to the water table is not visible above z_{wt}, while the one originated at the surface is visible at all depths, although it is relatively weak. The behavior for the IRs of both fields confirms the numerical results we obtained in our previous work (Zyserman et al., 2017). The coseismic magnetic field H-Cos shows the same behavior than the electric coseismic field E-Cos. However, for the magnetic field the coseismic response and the interfacial response have the same amplitude below the water table.

Finally, we explore the dependence of the electromagnetic responses on the saturation S_w of medium 1. Because of the lack of space, no figure is included, but we observe that an increase in the saturation will produce an increase in the amplitude of E-IR and H-IR at the surface together with a decrease in the amplitude of E-IR and H-IR at z_{wt}.

CONCLUSIONS

The derived solution provides new mathematical expressions to analytically study the dependence of the seismoelectromagnetic interface and coseismic responses with the physical parameters of the media. An important feature of the solution is that the interfacial and coseismic responses are explicit in the field's mathematical expressions, so they can be analyzed separately. Finally, the obtained results are in complete agreement with our previous work, showing that a sharp contrast in water saturation at the water table can induce strong interfacial responses in both fields, and in the case of the electric field, the amplitude of the interfacial response is three orders of magnitude higher than the coseismic response.

REFERENCES

Dupuis, J. C., Butler, K. E., Kepic, A. W., and Harris, B. D., oct 2009, Anatomy of a seismoelectric conversion: Measurements and conceptual modeling in boreholes penetrating a sandy aquifer: J. Geophys. Res. Solid Earth, **114**, no. B13, B10306.

Guan, W., Hu, H., and Wang, Z., 2013, Permeability inversion from low-frequency seismoelectric logs in fluid-saturated porous formations: Geophysical Prospecting, **61**, 120–133.

Haines, S. H., and R.Pride, S., 2006, Seismoelectric numerical modeling on a grid.:

Geophysics, **71**, 57–65.

Liu, X., and Greenhalgh, S., 2014, Reflection and transmission coefficients for an incident plane shear wave at an interface separating two dissimilar poroelastic solids: Pure Appl. Geophys., **171**, 2111–2127.

Pride, S., 1994, Governing equations for the coupled electromagnetics and acoustics of porous media: Phys. Rev. B: Condens. Matter, **50**, 15678–15695.

Pride, S., 2005, Relationships between the electrical and hydrogeological properties of rocks and soils *in* Rubin, Y., and Hubbard, S. S., Eds., Hydrogeophysics:: Springer, 87–128.

Schakel, M., Smeulders, D., Slob, E., and Heller, H., 2012, Seismoelectric fluid/porous-medium interface response model and measurements: Transport in Porous media, **93**, 271–282.

Valuri, J., Dean, T., and Dupuis, J., Brisbane, Australia 2012, Seismoelectric acquisition in an arid environment: 22nd Internat. Geoph. Conf. and Exhib.

Warden, S., Garambois, S., Jouniaux, L., Brito, D., Sailhac, P., and Bordes, C., 2013, Seismoelectric wave propagation numerical modeling in partially saturated materials: Geophys. J. Int., **194**, 1498–1513.

Zyserman, F., Gauzellino, P., and Santos, J., 2012, Numerical evidence of gas hydrate detection by means of electroseismics: J. Applied Geophysics, **86**, 98–108.

Zyserman, F., Jouniaux, L., Warden, S., and Garambois, S., 2015, Borehole seismoelectric logging using a shear-wave source:Possible application to CO_2 disposal?: International Journal of Greenhouse Gas Control, **33**, 82–102.

Zyserman, F. I., Monachesi, L. B., and Jouniaux, L., 2017, Dependence of shear wave seismoelectrics on soil textures: a numerical study in the vadose zone.: Geophysical Journal International, **208**, 918–935.